

Cell Reports, Volume 19

Supplemental Information

In Vivo DNA Re-replication

Elicits Lethal Tissue Dysplasias

Sergio Muñoz, Sabela Búa, Sara Rodríguez-Acebes, Diego Megías, Sagrario Ortega, Alba de Martino, and Juan Méndez

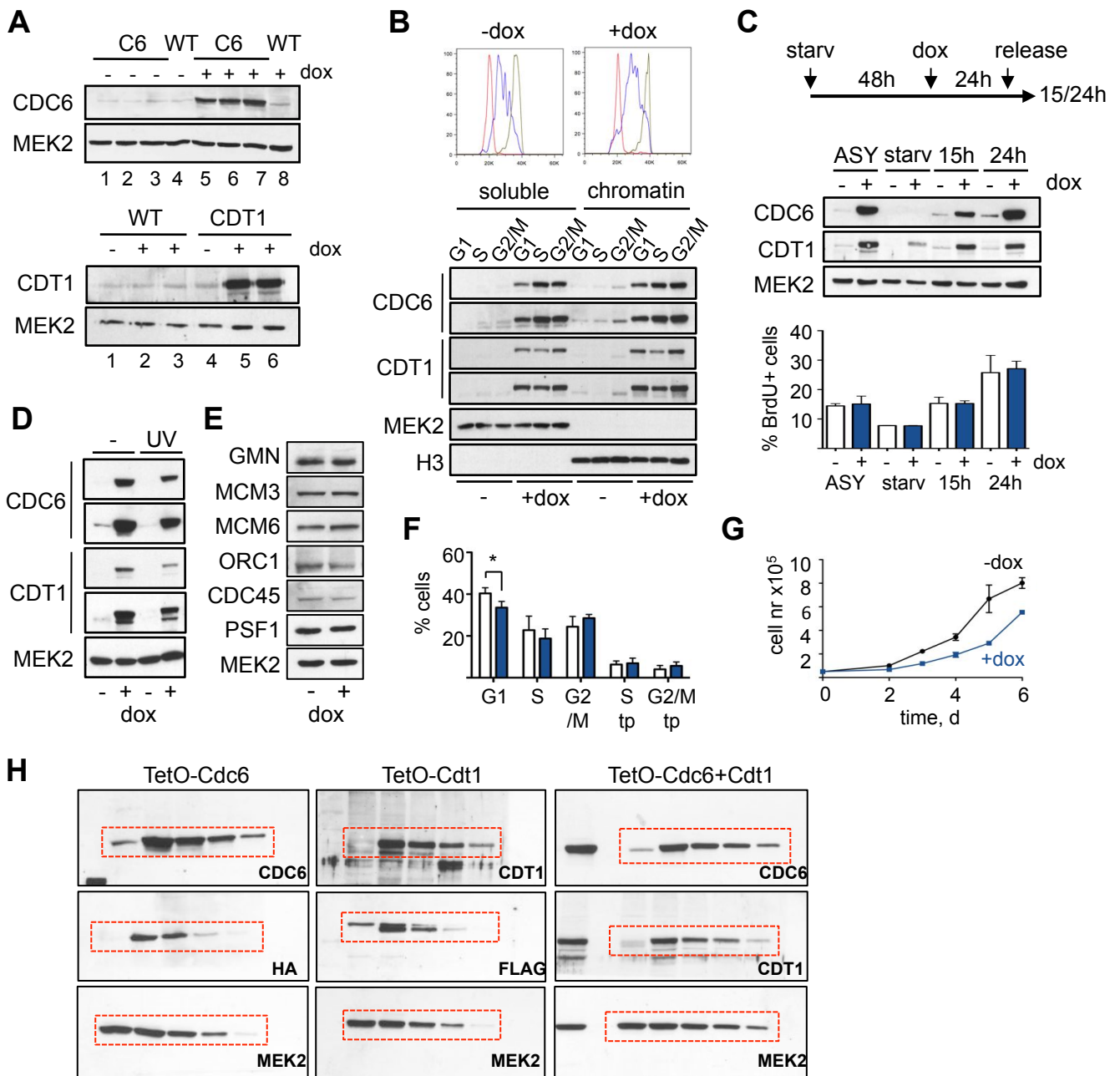


Figure S1. Cell cycle regulation of exogenous CDC6 and CDT1 proteins, Related to Figure 1. **A.** Top, CDC6 levels in WT (lanes 4,8) and 3 TetO-Cdc6 (C6) MEF isolates (lanes 1-3, 5-7). Bottom, CDT1 levels in WT or TetO-Cdt1 MEFs grown in control medium (lanes 1, 4) or in the presence of dox (2µg/ml, lanes 2, 5; 4µg/ml, lanes 3, 6) for 24 h. MEK2, loading control. **B.** Top, overlapping DNA content profiles of TetO-Cdc6+Cdt1 MEFs sorted in G1 (red), S (blue) or G2/M (green). Bottom, soluble and chromatin-bound proteins in each phase of the cell cycle. For CDC6 and CDT1, two exposures are shown. MEK2 and H3 are controls of the biochemical fractionation. **C.** Serum starvation and release in TetO-Cdc6+Cdt1 cells. CDC6 and CDT1 levels are shown in asynchronous (ASY) cells, serum-starved (starv) cells, and 15-24h post-release. MEK2, loading control. The percentage of cells positive for BrdU in each condition is quantified. **D.** CDC6 and CDT1 detection in TetO-Cdc6+Cdt1 MEFs after irradiation with 50 J/m² UV. Two exposures are shown. MEK2, loading control. **E.** Levels of the indicated proteins in the TetO-Cdc6+Cdt1 MEF extracts shown in Main Figure 2C. **F.** Percentage of TetO-Cdc6+Cdt1 MEFs in different phases of the cell cycle. White bar, control medium. Blue bars, medium supplemented with dox for 24 h (n=3 MEF isolates; *, p<0.05 in Student's T-test). tp=tetraploid. **G.** Proliferation curves of TetO-Cdc6+Cdt1 cells cultured without or with dox (n=2 assays). **H.** Uncropped films corresponding to immunoblots shown in Main Figure 1C. Cropped areas are marked in red dashed boxes.

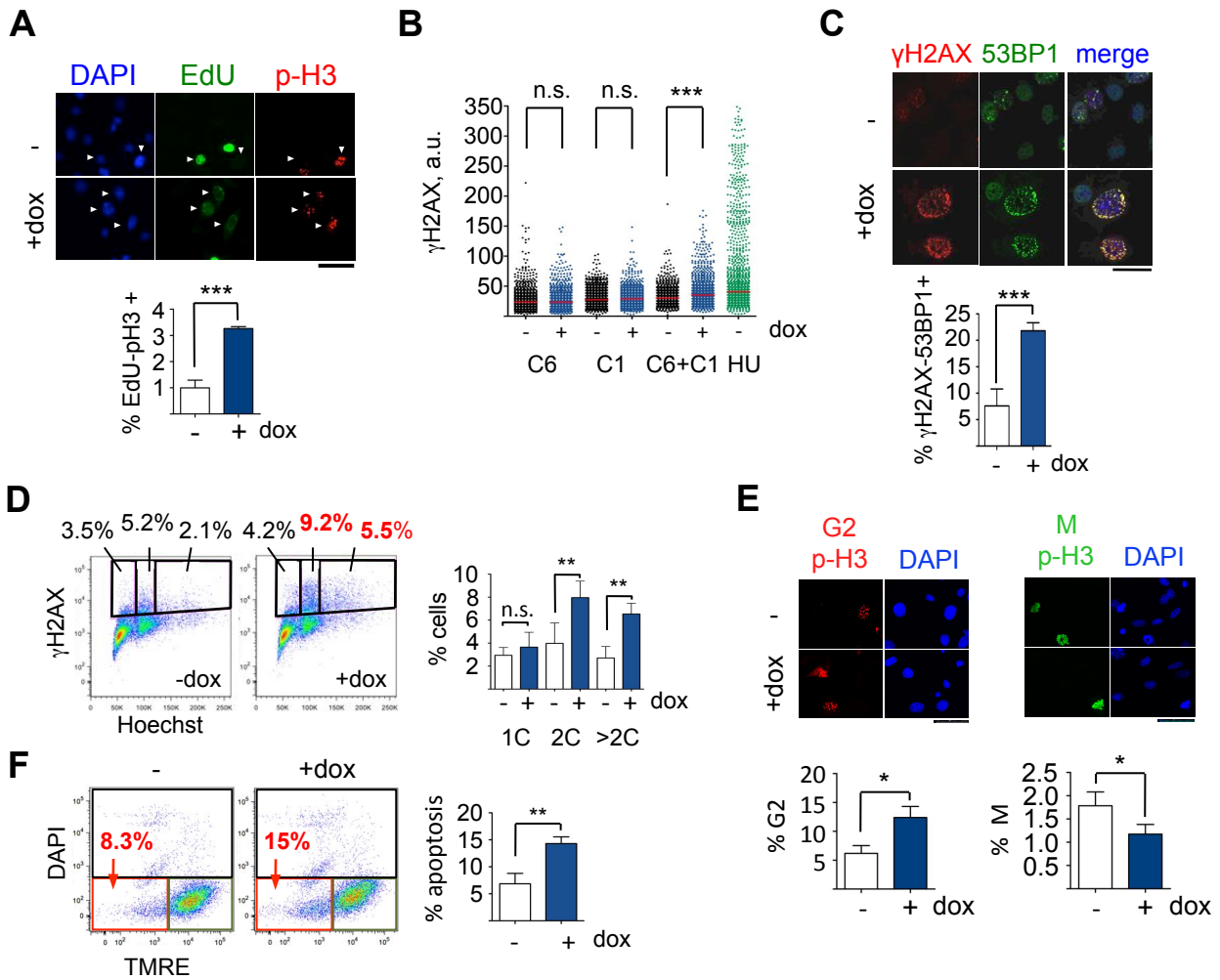


Figure S2. Unscheduled DNA replication in G2, DDR activation and apoptosis, Related to Figure 2. A.

Representative images of TetO-Cdc6+Cdt1 MEFs, pulse-labeled with EdU and immunostained for p-H3. DNA was counterstained with DAPI. Bar, 50 μ m. Histogram shows the percentage (mean and SD) of cells positive for EdU and G2-pattern p-H3 (n=4, >500 cells/condition scored in each assay; ***, p<0.001 in Student's T-test). **B.** HTM acquisition of γ H2AX fluorescence intensity in the indicated MEFs. Positive control, 2.5 mM HU for 3h (green). A representative assay is shown (n=3 assays; >1000 nuclei/condition in each assay; ***, p<0.001; n.s., not significant in Kruskal-Wallis test followed by Dunn's post-test). **C.** Representative images of TetO-Cdc6+Cdt1 cells immunostained for γ H2AX and 53BP1. DNA was counterstained with DAPI (blue). Bar, 25 μ m. Histogram shows the percentage (mean and SD) of cells positive for γ H2AX and 53BP1 foci (n=3 assays; >500 nuclei/condition in each assay; ***, p<0.001 in Fisher's exact test). **D.** Flow cytometry analysis of γ H2AX vs DNA content in TetO-Cdc6+Cdt1 MEFs. Gates indicate γ H2AX-positive cells with DNA content 1C, 2C and >2C. Histogram shows percentage (mean and SD) of positive cells in each gate (n=3 assays; **, p<0.01; n.s., not significant in one way Anova and Bonferroni's post-test). **E.** Representative images and quantification of TetO-Cdc6+Cdt1 MEFs displaying G2- (left) or M-characteristic (right) p-H3 staining patterns. DNA was counterstained with DAPI. Bar, 50 μ m. Histograms show the percentage (mean and SD) of positive cells (n=3 assays. >500 cells/condition scored in each assay for G2 pattern; >1000 cells/condition scored in each assay for mitotic pattern. *, p<0.05 in Student's t-test). **F.** Detection of apoptotic cells in TetO-Cdc6+Cdt1 MEFs after dox treatment (48 h). Left, flow cytometry plots of DAPI vs TMRE. Dead cells are included in the top gate, apoptotic cells in the bottom left gate (red), and living cells in the bottom right gate. Histogram shows percentage of apoptotic cells. (n=3; **, p<0.01 in Student's t-test).

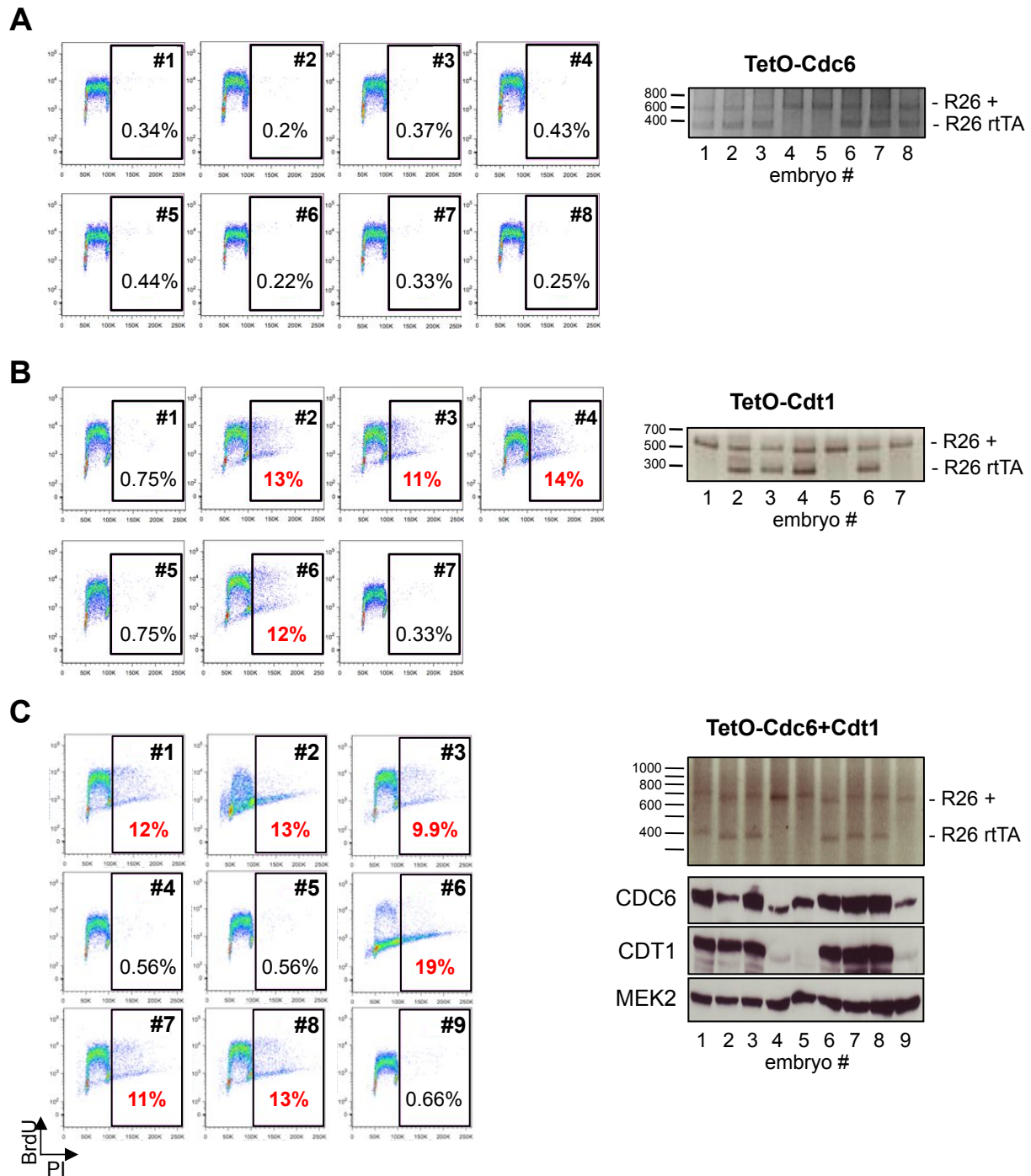
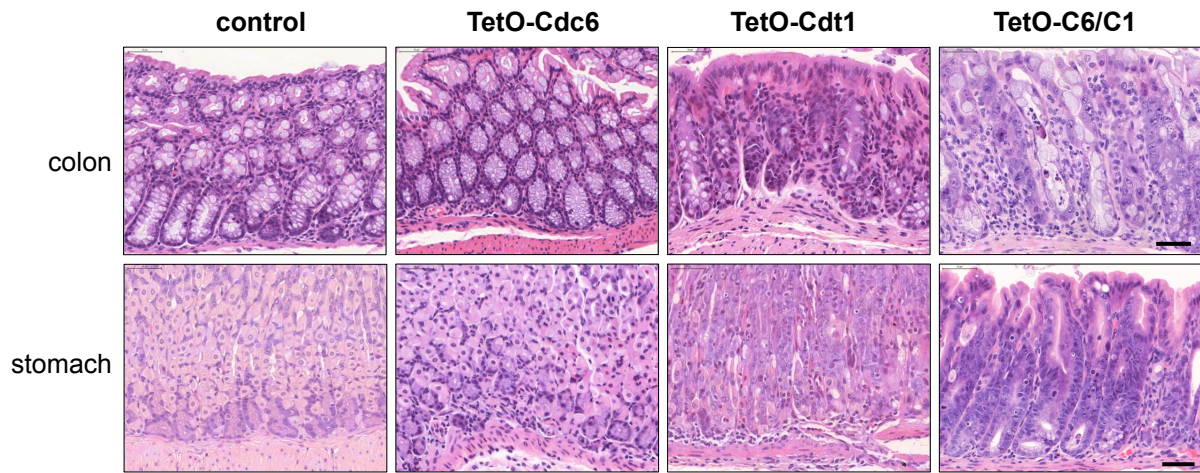


Figure S3. Deregulation of Cdt1 induces re-replication in embryos, Related to Figure 2. **A.** The experiment follows the outline described in Figure 2D, using fetal liver cells isolated from 8 TetO-Cdc6 littermate embryos of which 50% are predicted to overexpress Cdc6. Fetal liver cells were pulse-labeled *ex vivo* with BrdU for 30 min. Gates show cells with >2C DNA content. Right, PCR genotype indicates the presence or absence of rtTA at Rosa26, characteristic of overexpressors. **B.** Same as (A), using 7 embryos derived from TetO-Cdt1 mice. **C.** Same as (A), using 9 embryos derived from TetO-Cdc6+Cdt1 mice. CDC6 and CDT1 protein levels in total embryonic tissue are shown.

A



B

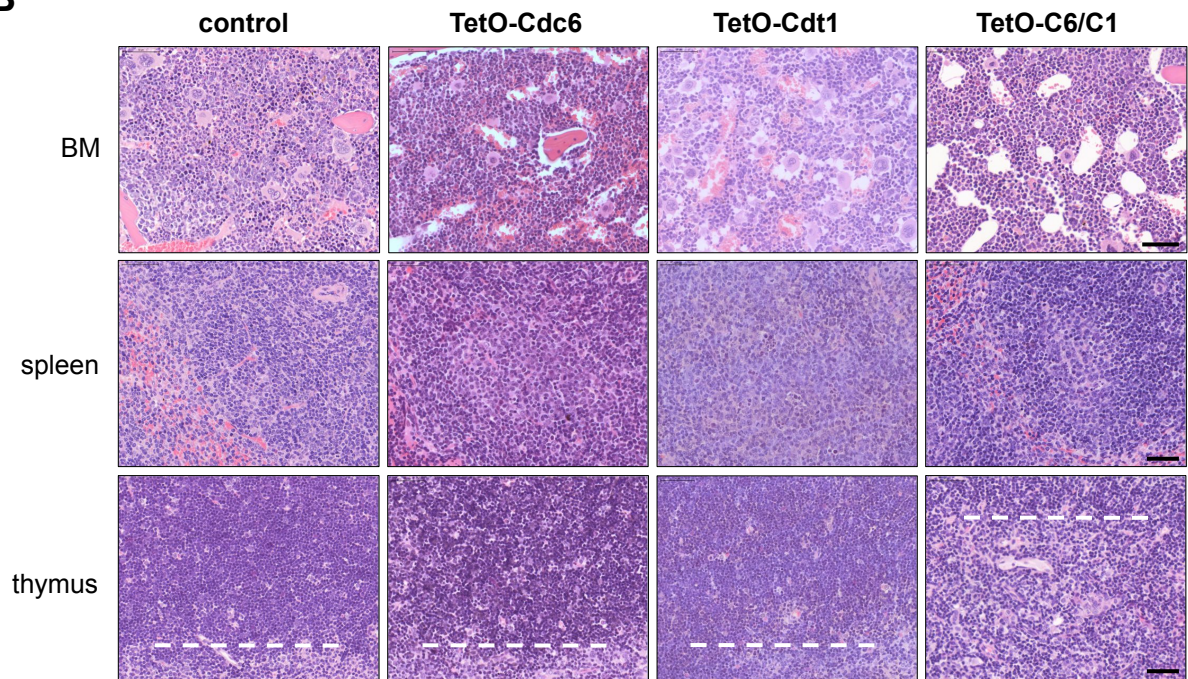


Figure S4. Tissue abnormalities caused by Cdc6 and Cdt1 deregulation, Related to Figure 3. A. Hematoxylin-eosin stainings in colon and stomach sections of control (untreated) or dox-treated TetO-Cdc6, TetO-Cdt1 and TetO-Cdc6+Cdt1 mice. Top-left and top-right images are shown at higher magnification in Figure 3D. **B.** Hematoxylin-eosin stainings in bone marrow (BM), spleen and thymus sections of the same mice. In the thymus, the boundary between cortical (top) and medullar (bottom) tissue is indicated by dashed lines. Bars, 50 μ m.

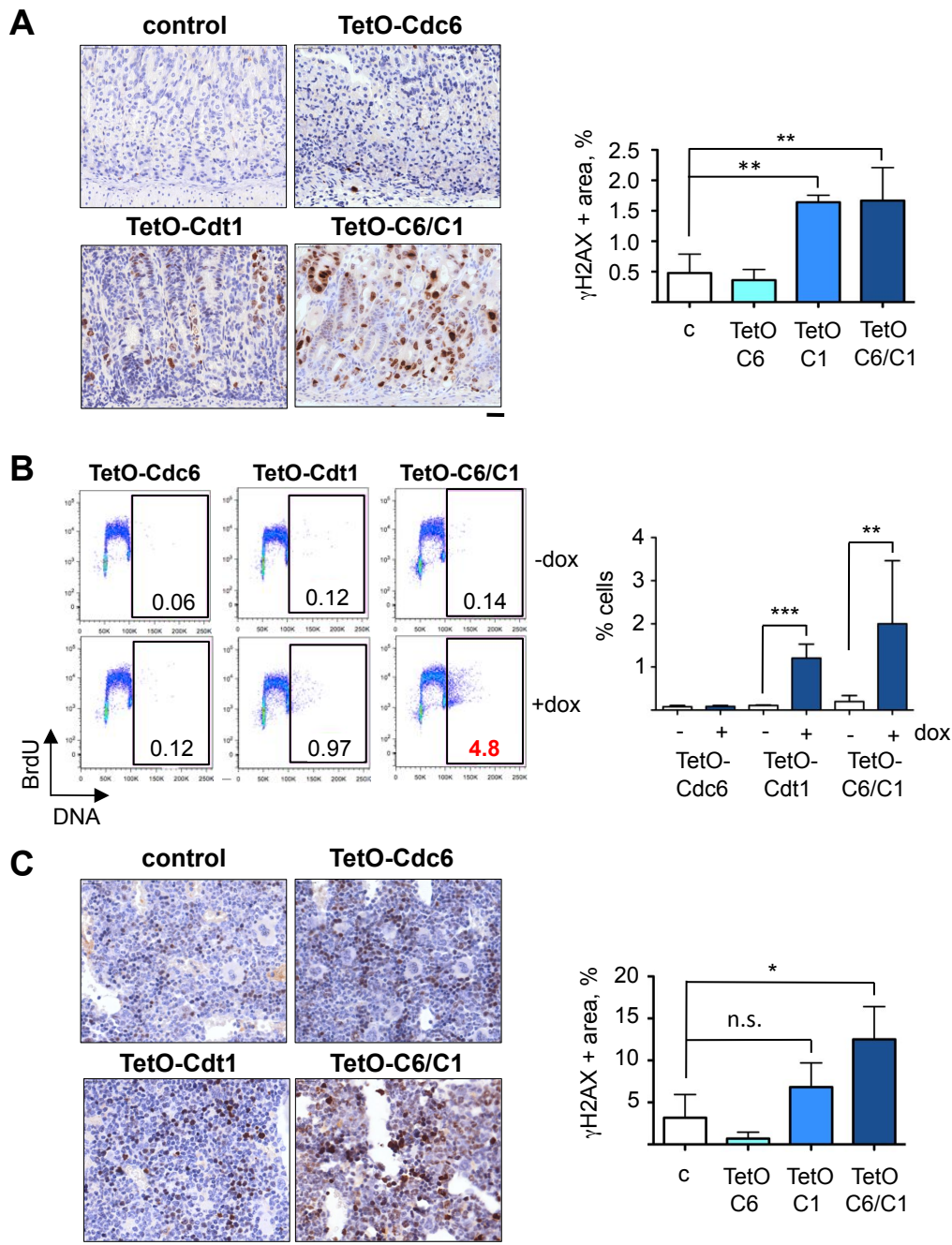


Figure S5. DNA re-replication and DNA damage in stomach and BM, Related to Figure 3. **A.** γ H2AX IHC staining in stomach tissue sections of control or dox-treated TetO-Cdc6, TetO-Cdt1 and TetO-Cdc6+Cdt1 mice. Histogram shows the percentage (mean and SD) of γ H2AX-positive area in each case. (**, $p < 0.01$ in one way Anova and Bonferroni's post-test). **B.** Flow cytometry profiles of BrdU incorporation vs DNA content in BM cells isolated from control or dox-treated TetO-Cdc6, TetO-Cdt1 and TetO-Cdc6+Cdt1 mice. Cells were pulse-labeled *ex vivo* with BrdU for 30 min. Gates include cells with $>2C$ DNA content. Histogram shows the percentage (mean and SD) of cells with $>2C$ DNA content ($n=4$ mice/strain and condition; ***, $p < 0.001$; **, $p < 0.01$; n.s., not significant, in one way Anova and Bonferroni's post-test). **C.** γ H2AX IHC staining in BM tissue sections of the same mice used in (A). Histogram shows the percentage (mean and SD) of cells with $>2C$ DNA content. (*, $p < 0.05$; n.s., not significant in one way Anova and Bonferroni's post-test).

Supplemental Experimental Procedures

Generation of TetO-Cdc6, TetO-Cdt1 and TetO-Cdc6+Cdt1 mouse strains

DNAs coding for HA-tagged CDC6 and Flag-tagged CDT1 were obtained by PCR from the mouse Cdc6 and Cdt1 cDNAs (IMAGE Consortium clones #6837113 and #6307476, respectively) and inserted individually in plasmid pBS31 (Beard et al, 2006). KH2 embryonic stem cells were co-transfected with either pBS31-HA-Cdc6 or pBS31-Cdt1-FLAG and a vector expressing FlpE recombinase. Genomic integration was confirmed by Southern blot and positive KH2 clones were used for ES cell aggregation. The rtTA transgene at Rosa26 was maintained in heterozygosis.

Antibodies

Primary antibodies and dilutions used for immunoblotting: ORC1 (Méndez et al, 2002; 1:200 dilution); MCM2 (Ekholm-Reed et al, 2004; 1:1000); MCM3 and MCM4 (Alvarez et al, 2015; 1:1000); CDC45 and PSF1 (Aparicio et al, 2009; 1:500). Commercial antibodies: CDC6 (Millipore 05-550; 1:500); CDT1 (Millipore 07-1383; 1:1000); HA (Cell Signaling 2367; 1:500); FLAG (Cell Signaling 2368; 1:1000); MEK2 (BD Biosciences Pharmingen 610236; 1:2000); SMC1 (Bethyl A300-055A; 1:1000); γ H2AX (Millipore 05-636; 1:200); GMN (Santa Cruz sc-13015; 1:1000); pS15-p53 (Cell Signaling 92845; 1:500); pTyr15-CDK1 (Cell Signaling 9111; 1:1000). Antibodies for immunofluorescence, flow cytometry and single-molecule analyses of DNA replication: FITC-conjugated BrdU (BD Pharmingen 556028; 1:50), CldU (rat monoclonal anti-BrdU, Abcam ab6326; 1:100), IdU (mouse monoclonal anti-BrdU, BD 347580; 1:100), ssDNA (Millipore MAB3034; 1:100), pSer10-H3 (Abcam ab14955; 1:200), 53BP1 (Novus Biologicas NB-100-304; 1:500). Antibodies for IHC staining: γ H2AX (Millipore, 05-636; 1:100); Ki67 (Master Diagnostica 0003110QD; 1:500); SOX9 (Millipore AB5535; 1:800); pSer10-H3 (Millipore 06-570; 1:500); p21 and p16 (CNIO Monoclonal Antibody Unit; 1:10; cleaved caspase-3 (Cell Signaling Technology 9661; 1:750). Secondary antibodies for immunoblot: horseradish peroxidase-linked ECL anti-rabbit or anti-mouse IgG (NA934V, NA931V, GE Healthcare; 1:5000). Secondary antibodies for immunofluorescence: anti-rabbit IgG AF-488 (chicken) or AF-594 (goat); anti-mouse IgG AF-488 (goat) or AF-594 (donkey); anti-rat IgG AF-594 (goat); anti-mouse IgG2a AF-647 (goat): all from Invitrogen Molecular Probes (1:200).

Flow cytometry detection of BrdU incorporation, DNA content and apoptotic cells

MEFs were pulse-labeled with 10 μ M BrdU (Sigma) for 30 min. Fetal liver tissue from E13.5 embryos or adult femur BM were disaggregated in RPMI-2% FBS by passage through a 26G needle, filtered in a 70 μ m strainer (BD Falcon) and pulse-labeled with BrdU (30 min/ 37 C). Cells were fixed in 70% ethanol, treated with 2M HCl for 20 min and incubated with FITC-conjugated anti-BrdU antibody (60 min/ 37C). To monitor DNA content, cells were stained with 50 μ g/ml propidium iodide (PI; Sigma) in the presence of 10 μ g/ml RNase A (Qiagen). The crypt-enriched fraction of intestinal cells was isolated as described (Sato and Clevers, 2013) and stained with PI as above. For γ H2AX detection, MEFs were fixed with 4% PFA (15 min/ RT) and permeabilized with 0.5% Triton-X100 in PBS (10 min/ 4 C). Cells were incubated in blocking solution (1% bovine serum albumin in PBS; 0.05% Tween-20) for 15 min, followed by primary and secondary antibodies for 1 h at RT. DNA was stained with 5 μ g/ml Hoechst (Invitrogen).

For the quantification of dead and apoptotic cells, MEFs were harvested and incubated with 1 μ g/ml DAPI and 40 nM tetramethyl rhodamine ethylester (TMRE, Sigma) for 10 min at 37 C. Flow cytometry was performed in a FACS Canto II cytometer (BD) and data were analyzed with FlowJo 9.4 (Tree Star). Cell sorting was carried out in a BD Influx Sorter after DNA staining with 5 μ g/ml Hoechst (Invitrogen) for 30 min at 37 C.

Immunofluorescence microscopy and high-content image acquisition

MEFs cultured in polylysine-treated coverslips were fixed in 4% PFA (15 min/ RT) and permeabilized with 0.5% Triton-X100 in PBS (5 min/ RT). Coverslips were sequentially incubated in blocking solution (2% BSA in PBS), primary and secondary antibodies (1 h/ RT). Nuclear DNA was stained with 1 μ g/ml DAPI. Coverslips were mounted onto microscope slides using Mowiol (Calbiochem). For 53BP1 and γ H2AX co-immunostaining, soluble proteins were extracted prior to fixation with 0.5% Triton X-100 in CSK buffer (10mM Pipes-KOH pH 7.0; 100mM NaCl; 300mM sucrose; 3mM MgCl₂). EdU incorporation was monitored using the Click-iT EdU AF488 imaging kit (Invitrogen).

For High-Throughput Microscopy (HTM) assays, cells were cultured in μ CLEAR bottom polylysine-treated 96-wells (Greiner Bio-One) and analyzed in an Opera High-Content Screening System with an

APO 20x, 0.7 NA water-immersion objective (PerkinElmer). Nuclei were stained with DAPI, and the IF intensity of the indicated protein was measured within the nuclei mask using Acapella software (PerkinElmer). Intensity of chromatin-bound MCM was determined after pre-extraction of soluble proteins as described above.

Single-molecule analysis of DNA replication

For IOD and FR analyses, MEFs were pulse-labeled with 50 μ M CldU (20 min) followed by 250 μ M IdU (20 min). Labeled cells were resuspended in ice-cold PBS and lysed in 0.2 M Tris pH 7.4, 50 mM EDTA, 0.5% SDS (6 min/ RT). Microscope slides were tilted 15 degrees to spread DNA fibers. Slides were air-dried and fixed in methanol: acetic acid (3:1) for 2 min. DNA was denatured with 2.5 M HCl for 30 min at RT. Slides were incubated in blocking buffer (0.1% Triton X-100, 1% BSA in PBS) for 1 h/ RT. Following sequential incubation with primary (1h/RT) and secondary antibodies (30 min/RT), slides were air-dried and mounted with Prolong (Invitrogen). For analysis of origin re-firing, cells were pulse-labeled with 50 μ M CldU (2 h) followed by 250 μ M IdU (30 min) as described (Neelsen et al, 2013). In this case, DNA fibers were incubated in “stringency buffer” (10 mM Tris-HCl pH 7.4; 0.4 M NaCl; 0.2% Tween-20; 0.2% NP-40) for 10 min between primary and secondary antibodies, as described (Dorn et al, 2009). Images were obtained in a DM6000 B Leica microscope with an HCX PL APO 40x, 0.75 NA objective. Conversion factor 1 μ m = 2.59 kb was used (Jackson and Pombo, 1998).

Statistical Methods

Statistical analyses were performed in Prism v4.0 (GraphPad Software). In column histograms, data are expressed as mean and standard deviation (s.d.). In scattered dot plots, horizontal bars indicate the median value. When two data groups are compared, two-tailed unpaired Student’s t-test or Fisher’s exact test was used. For the analyses of FR or IOD in stretched DNA fibers, data distribution is normally not Gaussian, and statistical differences were assessed with nonparametric Mann-Whitney rank-sum test. For comparisons between multiple groups, one-way Anova test and Bonferroni’s post-test were applied. In HTM, we used the nonparametric Kruskal-Wallis test followed by Dunn’s post-test. The specific analysis used in each experiment is indicated in the corresponding Figure legend.

Supplemental References

- Aparicio T, Guillou E, Coloma J, Montoya G, Méndez J. 2009. The human GINS complex associates with Cdc45 and MCM and is essential for DNA replication. *Nucleic Acids Res* **37**: 2087-2095.
- Beard C, Hochedlinger K, Plath K, Wutz A & Jaenisch R. 2006. Efficient method to generate single-copy transgenic mice by site-specific integration in embryonic stem cells. *Genesis* **44**: 23-28.
- Dorn ES, Chastain PD, Hall JR, Cook JG. 2009. Analysis of re-replication from deregulated origin licensing by DNA fiber spreading. *Nucleic Acid Res* **37**: 60-69.
- Ekholm-Reed S, Méndez J, Tedesco D, Zetterberg A, Stillman B, Reed SI. 2004. Deregulation of cyclin E in human cells interferes with prereplication complex assembly. *J Cell Biol* **165**: 789-800.
- Jackson DA, Pombo A. 1998. Replicon clusters are stable units of chromosome structure: evidence that nuclear organization contributes to the efficient activation and propagation of S phase in human cells. *J Cell Biol* **140**: 1285-1295.
- Sato T, Clevers H. 2013. Primary mouse small intestinal epithelial cell cultures. *Methods in Molecular Biology* **945**: 319-328.